Nanoscale

PAPER

SiO₂ nanoparticles biocompatibility and their potential for gene delivery and silencing†

Maria Ada Malvindi,[a] Virgilio Brunetti,[a] Giuseppe Vecchio,[a] Antonio Galeone,[a] Roberto Cingolani[b] and Pier Paolo Pompa*[a]

Despite the extensive use of silica nanoparticles (SiO₂NPs) in many fields, the results about their potential toxicity are still controversial. In this work, we have performed a systematic *in vitro* study to assess the biological impact of SiO₂NPs, by investigating 3 different sizes (25, 60 and 115 nm) and 2 surface charges (positive and negative) of the nanoparticles in 5 cell lines (3 in adherence and 2 in suspension). We analyzed the cellular uptake and distribution of the NPs along with their possible effects on cell viability, membrane integrity and generation of reactive oxygen species (ROS). Experimental results show that all the investigated SiO₂NPs do not induce detectable cytotoxic effects (up to 2.5 nM concentration) in all cell lines, and that cellular uptake is mediated by an endocytic process strongly dependent on the particle size and independent of its original surface charge, due to protein corona effects. Once having assessed the biocompatibility of SiO₂NPs, we have evaluated their potential in gene delivery, showing their ability to silence specific protein expression. The results of this work indicate that monodisperse and stable SiO₂NPs are not toxic, revealing their promising potential in various biomedical applications.

Introduction

Silicon dioxide nanoparticles (SiO₂NPs) are widely used in various industrial fields, as additives to drugs, cosmetics, printer toners and food packaging applications. Recently, they have been exploited also for biomedical research, such as in cancer therapy,[1] DNA delivery[2] and enzyme immobilization.[3] Due to their wide range of applications, the impact of SiO₂NPs on human health and the environment is thus of great interest.[4–6] At the moment, there are only few studies investigating the toxic effects of SiO₂NPs, by far less than titanium dioxide NPs[7,8] or carbon nanotubes.[9,10] *In vitro* studies of SiO₂NPs indicate that the particle surface area as well as the particle size[11–14] or shape[15] may play a crucial role in the toxicity of nanosilica.[15,16] Surface silanol groups have been reported to be directly involved in hemolysis[17,18] and in alveolar epithelial cell toxicity.[19] Other parameters that deserve attention are the protein–SiO₂NP interactions, which appear to be affected by the size[20–22] and by the chemical modification of the nanoparticle surface that determines the interaction with the cell membrane, leading to a safe NPs uptake[14] or to a perturbation of the intracellular mechanisms.[6,22] Some *in vitro* studies have also emphasized that the response to SiO₂NPs varies as a function of the cell type.[14,23–25] The overall evaluation of the toxicity/biocompatibility of SiO₂NPs is, therefore, extremely difficult, owing to controversial results in the literature and to the lack of standard procedures and/or insufficient characterization of the nanomaterials in biological systems. The available data are not sufficient to clearly identify and characterize the biological effects of SiO₂NPs, and to define the appropriate conditions for a safe use of these nanomaterials. A crucial issue is the accurate physico-chemical characterization of the NPs such as size, dispersion, surface area and chemistry, stability and/or aggregation in biological media. Equally important is also the control of the assay conditions.[26,27] Biocompatibility needs to be documented in greater detail also because several biomedical applications of SiO₂NPs are emerging.[28–30]

The aim of this study is to perform a systematic investigation of the possible cytotoxicity caused by monodisperse and stable SiO₂NPs. We used five cell lines, both in adherence (A549, HeLa, and Caco-2) and in suspension (U937 and Jurkat); three different sizes of SiO₂NPs: 25, 60 and 115 nm; two surface charges (negative and positive) and three different cytotoxicity tests: the WST-8 assay (cell viability), the LDH assay (cell membrane integrity), and the DCF assay (ROS level). The cellular uptake of the different nanoparticles was also examined. Finally, having

a Italian Institute of Technology, Center for Bio-Molecular Nanotechnologies@Unile, Via Barsanti, 73010 Arnesano, Lecce, Italy. E-mail: pierpaolo.pompa@iit.it; Fax: +39-0832-295708; Tel: +39-0832-295714
b Italian Institute of Technology, Central Research Laboratories, Via Morego, 30, 16136, Genova, Italy

demonstrated that SiO₂NPs do not cause toxic effects, an efficient gene delivery system based on the SiO₂NPs was demonstrated.

Results and discussion

Stable and monodisperse silica nanoparticles of different sizes (25, 60, and 115 nm) were synthesized through the microemulsion method[31] and their physico/chemical properties were accurately characterized by different techniques. Nanoparticles showed highly uniform morphology and size dispersion, without shape irregularities on their surface, as confirmed by TEM images (Fig. 1). The stability of the nanoparticle suspensions was investigated by monitoring the particle size directly in solution, using dynamic light scattering (DLS), and the surface charge through ζ-potential measurements (see the table in Fig. 1). The hydrodynamic sizes of SiO₂NPs turned out to be consistent with the TEM data. ζ-Potential measurements documented the negative surface charge related to the silanol groups, whereas SiO₂NPs with amine groups, treated with aminopropyltriethoxysilane (APTES), yielded positively charged nanoparticles.

Cellular experiments were carried out to examine the effects of SiO₂NP size and surface charge on cellular uptake and toxicity. We evaluated three cytotoxicity parameters, namely (i) cell viability with the WST-8 assay, (ii) cell membrane integrity with the LDH assay, and (iii) the generation of ROS with the DCF assay. We investigated a wide range of concentration (up to 2.5 nM) and incubation time (up to 96 h). The amount of SiO₂NPs internalized by cells was determined through elemental analysis by inductively coupled plasma atomic emission spectroscopy (ICP-AES).

Cell viability was evaluated both in terms of dose- and time-dependence by measuring the reduction of WST-8 as marker of changes in the metabolic activity. Experiments were performed at 48 and 96 h, testing four SiO₂NP concentrations: 2.5, 25, 250, and 2500 pM (respectively, S1, S2, S3, and S4). As a representative example, in Fig. 2 we display the cell viability after treatment with SiO₂NPs of 25 nm diameter. Upon exposure to increasing doses of SiO₂NPs, the viability of A549, HeLa, Caco-2, U937 and Jurkat cells was evidently not altered up to 96 h, regardless of the NPs surface charge. The same non-toxic behavior was observed for the other two sizes (Fig. S1 and S2†). Despite size-dependent cytotoxicity of SiO₂NPs having been previously reported (smaller particles were found to be more toxic),[13,32] our data showed no viability reduction, likely due to the lower NP concentrations used in our experiments.

The uptake of nanoparticles can affect the cell membrane integrity. Therefore, we assessed the effect of SiO₂NPs on cell
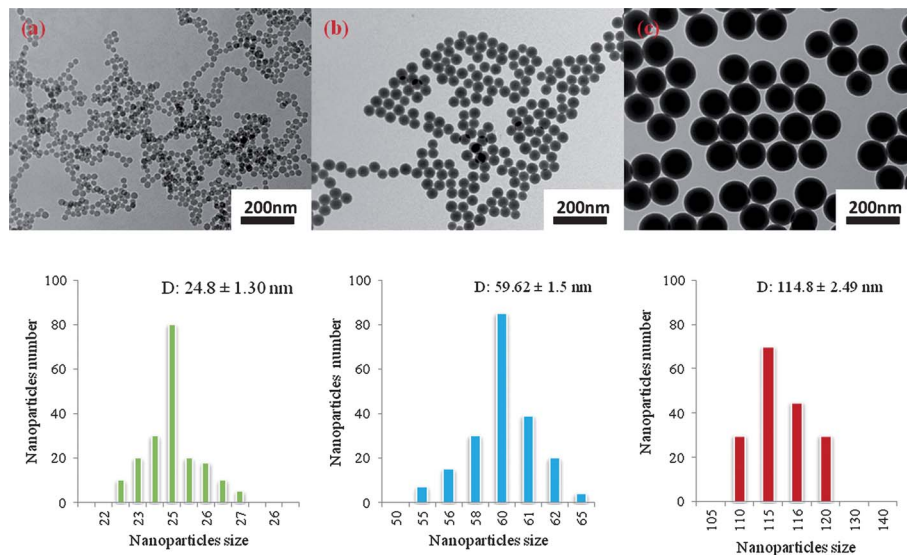
	DLS (nm)	ζ-Potential (mV)
SiNPs 25 (-)	25 ± 2 nm	-26 ± 6 mV
SiNPs 25 (+)	25 ± 4nm	+30 ± 5 mV
SiNPs 60 (-)	67 ± 1 nm	-28 ± 5 mV
SiNPs 60 (+)	68 ± 1 nm	+32 ± 5 mV
SiNPs 115 (-)	138 ± 4 nm	-45 ± 6 mV
SiNPs 115 (+)	138 ± 4 nm	+52 ± 5 mV

Fig. 1 From the top: TEM images of SiO₂NPs of different sizes, namely (a) 24.8 ± 1.3 nm, (b) 59.62 ± 1.5 nm and (c) 114.8 ± 2.49 nm. Size distributions of SiO₂NPs after measuring the size of more than 100 particles by TEM. Dynamic light scattering and ζ-potential measurements of negatively and positively charged SiO₂NPs.
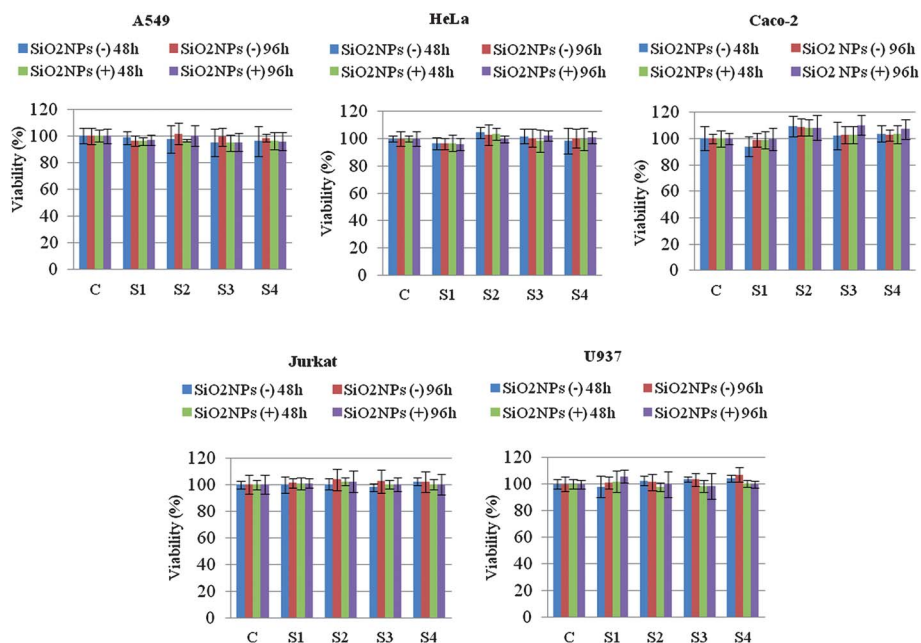
Fig. 2 Viability of A549, HeLa, Caco-2, U937, and Jurkat cells 48 and 96 h after the exposure to increasing doses (S1: 2.5 pM, S2: 25 pM, S3: 250 pM, and S4: 2500 pM) of SiO$_2$NPs (diameter 25 nm) evaluated by the WST-8 assay. Viability of nanoparticle-treated cells is expressed relative to non-treated control cells. As a positive control, cells were incubated with 5% DMSO (showing a viability decrease of *ca.* 50%). Error bars indicate the standard deviation.

membrane integrity by the LDH leakage assay, using the highest concentration of NPs (2.5 nM). We did not observe any detectable release of LDH over 96 h (Fig. 3). All cell lines proved to be insensitive to all the NPs tested, in terms of membrane damage, unlike previous findings reporting size-dependent membrane

damage in cells, but again at significantly higher concentrations.[32]

Oxidative stress has been suggested, also, to play an important role in the mechanism of toxicity. Although some studies showed that SiO$_2$NPs may induce increased ROS levels,[32] in this study,
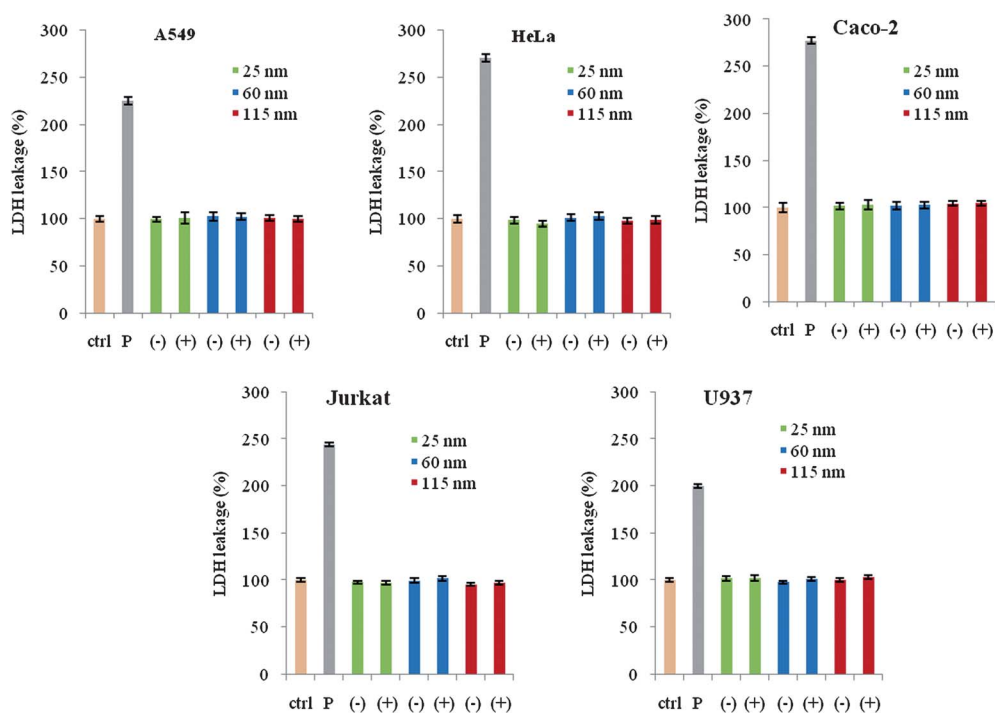
Fig. 3 LDH release in the five cell lines after 96 h exposure to the three sizes (25, 60 and 115 nm) of silica nanoparticles and two surface charges (negative and positive) at the highest concentration (2.5 nM). Percentage of LDH leakage of nanoparticle-treated cells is expressed relative to non-treated control cells. Positive controls (P) consisted in the treatment of cells with 0.9% Triton X-100. Error bars indicate the standard deviation.

even the highest NP concentration (2.5 nM) did not produce detectable ROS increase over 96 h in any cell lines, for any size and surface charge of SiO₂NPs (Fig. 4). Overall, the above results consistently indicate that SiO₂NPs of 25, 60 and 115 nm do not cause cytotoxicity effects, when used at concentration less than 2.5 nM.

The uptake and distribution of SiO₂NPs were assessed by confocal microscopy and ICP-AES measurements. For confocal imaging, we used SiO₂NPs doped with QDs (CdSe/ZnS). The physico-chemical properties of the doped 25 nm particles are reported in Fig. S3†. Also in this case, we evaluated the biocompatibility of these nanosystems finding no signs of cytotoxicity (no detectable variations in cell viability, membrane damage or ROS levels, Fig. S4–S6†). This suggests that the thick silica shell around the QDs prevents their toxicity, likely reducing Cd^+ ion release. As a representative image, the distribution of 25 nm SiO₂NPs in cell is shown in Fig. 5. A typical cytoplasmatic/perinuclear distribution was observed, with the presence of some intracellular aggregates. A similar intracellular distribution was found for the other two sizes (60 and 115 nm).

To quantify the amount of SiO₂NPs taken up by cells and to clarify the possible dependence of NPs uptake on surface charge[33,34] and size,[35,36] elemental analysis was performed on two cell lines. We selected both adherent (A549) and suspension (Jurkat) cell lines. The cellular uptake of the NPs was monitored after 48 h and 96 h (since the same behavior was observed, we reported here only the results of 96 h). As expected, the smallest SiO₂NPs showed the highest internalization efficiency, followed by the 60 nm and 115 nm (Fig. 6). This behavior was observed in both cell lines, confirming the size-dependence as a quite general rule of NPs uptake. Interestingly, concerning the effect of the NPs surface charge on the uptake, we did not observe any significant difference in the internalization between negatively and positively charged SiO₂NPs. In both cell lines and for all the

three NP sizes, the values of NPs uptake were very similar, independent of the NPs surface charge. This is consistent with recent findings with gold[37] and silica nanoparticles.[38] Although on the basis of some studies, a "general rule" of higher cellular internalization of cationic NPs has been suggested, such a principle suffers some experimental limitations and is in evident contrast with the concept of protein corona, whose key role has been recently demonstrated in many experiments.[39,40] As soon as the NPs enter in contact with the cell culture media, they are immediately covered by a dynamic layer of serum proteins, so that the original size and surface charge of the NPs undergo significant changes.[41,42] We characterized the protein/NP entities formed upon incubation of our SiO₂NPs in the cell culture media (DMEM and RPMI), namely in the same conditions used in the cellular uptake experiments (with A549 and Jurkat, respectively). The hydrodynamic diameter increased for all the SiO₂NPs in both cell culture media, regardless of the positive or negative charge of the original surface. Generally, the SiO₂NPs suspended in DMEM presented a higher increase of the hydrodynamic diameter than those in RPMI, in agreement with previous findings.[41] We observed that the diameter increase was proportional to the particle dimension; such a size increase is due to the formation of protein corona around the NPs, which is also responsible for the change of the surface charge (all the NPs in both culture media acquired a negatively charged surface) (Fig. 6, bottom). The similar values of size and surface charge of the NPs in the cell culture medium well explain the observed uptake data.

To further clarify the internalization mechanism of these particles, we examined the effect of different inhibitors on the cellular uptake of SiO₂NPs. A549 cells were incubated with two metabolic inhibitors, namely sodium azide and 2-deoxyglucose. Sodium azide is widely used as an inhibitor of cellular respiration, decreasing intracellular ATP concentration.[43,44]
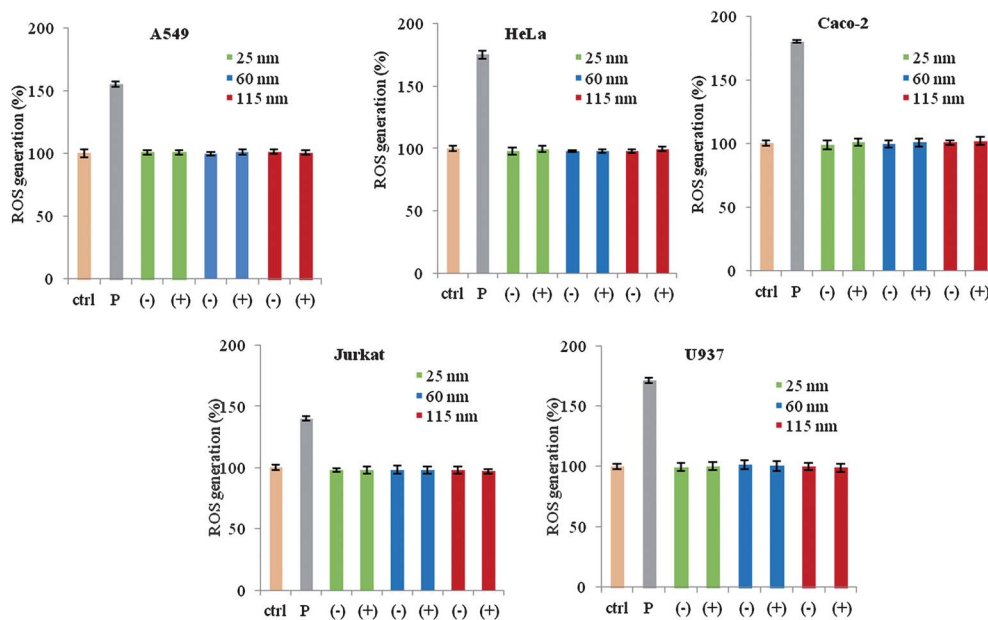

Fig. 4 Effects of SiO₂NPs on the level of ROS in five cell lines, probed by the DCFH-DA assay. Cells were treated with the highest concentration (2.5 nM) of NPs for 96 h. The ROS level of nanoparticle-treated cells is expressed relative to non-treated control cells. As a positive control (P), cells were incubated with 500 μM H₂O₂. Error bars indicate the standard deviation.
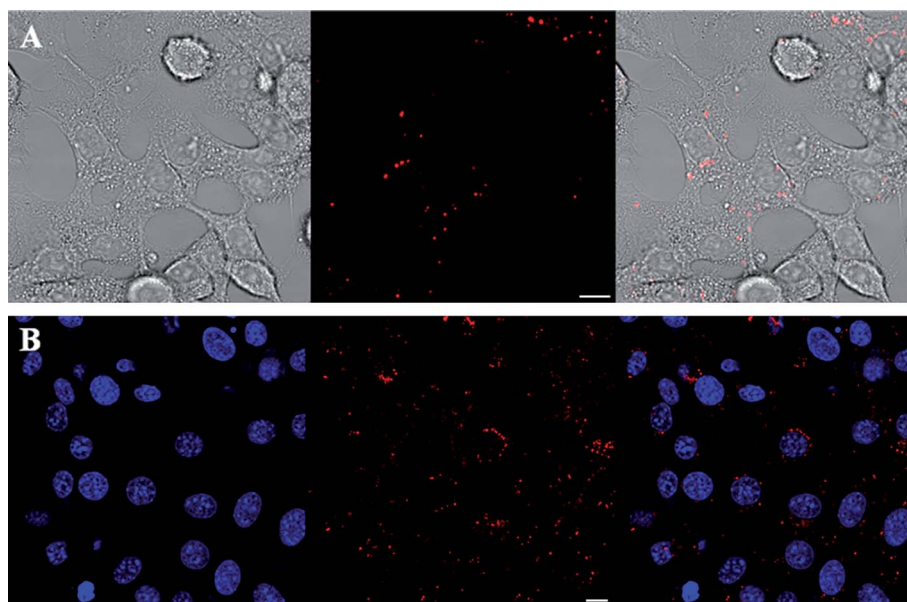
Fig. 5 Representative confocal images of A549 cells treated for 48 h with 10 nM 25 nm SiO$_2$NPs doped with QDs. (A) Left panel: transmission image; center panel: QDs fluorescence image; and right panel: merged image. (B) Left panel: nuclear staining; center panel: QDs fluorescence; and right panel: merged image. Scale bars: 10 μm.

2-Deoxyglucose is a glucose analog and acts as a competitive inhibitor of glucose. 2-Deoxyglucose is trapped and accumulated in the cells, leading to inhibition of glycolysis, through a depletion of cellular ATP, leading to blockage of cell cycle progression and cell death *in vitro*.[44,45] Both these inhibitors block the energy-dependent process of endocytosis. The uptake of SiO$_2$NPs was examined using elemental analysis by ICP-AES. Preincubation with the different metabolic inhibitors was observed to significantly reduce the uptake of SiO$_2$NPs by A549 cells, independently of the NPs surface charge. In Fig. 7 we reported the experimental data obtained in the case of 25 nm NPs, negatively and positively charged. Treatment with the inhibitors reduced
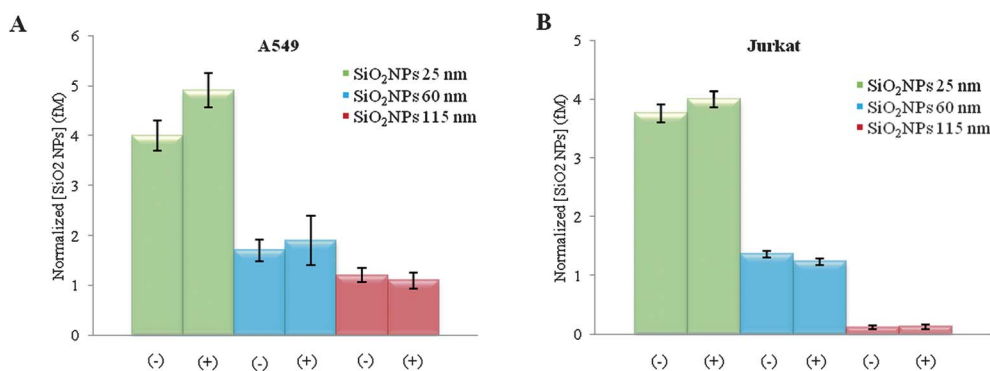
	DMEM		RPMI	
	DLS (nm)	ζ-Potential (mV)	DLS (nm)	ζ-Potential (mV)
SiO$_2$NPs 25 (-)	100 ± 15	-21 ± 6	87 ± 14	-19 ± 5
SiO$_2$NPs 25 (+)	100 ± 20	-25 ± 5	90 ± 17	-20 ± 3
SiO$_2$NPs 60 (-)	130 ± 16	-24 ± 5	90 ± 15	-23 ± 4
SiO$_2$NPs 60 (+)	131 ± 20	-34 ± 5	100 ± 20	-26 ± 3
SiO$_2$NPs 115 (-)	180 ± 18	-24 ± 6	135 ± 10	-23.5 ± 4
SiO$_2$NPs 115 (+)	250 ± 22	-38 ± 5	170 ± 19	-28 ± 5

Fig. 6 Amount of internalized SiO$_2$NPs (per cell), determined by ICP-AES after 96 h of incubation. (A) A549 cells (in DMEM) and (B) Jurkat cells (in RPMI). Bottom: ζ-Potential and dynamic light scattering measurements of different sizes of SiO$_2$NPs with different surface charges suspended in DMEM or RPMI culture medium for 96 h.

SiO$_2$NPs uptake of about 90%. The same results were observed with the other two sizes (60 and 115 nm), suggesting that all the SiO$_2$NPs are taken up by the cells mostly through an energy-dependent endocytic pathway.[46] The similar behavior exhibited in these experiments by positively and negatively charged NPs further confirmed the protein corona mediated cellular uptake of NPs discussed above.

After the experimental assessment of the *in vitro* biocompatibility of SiO$_2$NPs through the different assays, we evaluated their ability to act as transfection agents for gene delivery. So far, several strategies have been explored for *in vitro* and *in vivo* gene silencing. For instance, cationic polymeric nanoparticles[47] and cationic liposomal nanoparticles[48] were used to deliver siRNA. Recently, silica nanoparticles, encapsulating QDs and surface-functionalized with amino groups, have been shown to efficiently bind and delivery DNA.[49] Similar to this latter approach, we adsorbed electrostatically on the surface of 25 nm SiO$_2$NPs modified with amine groups, a plasmid vector containing a short hairpin RNA (shRNA) sequence targeting TurboGFP, an improved variant of the green fluorescent protein CopGFP. The conjugation conditions were optimized using two concentrations (0.5 and 2 μg) of the plasmid vector. The resulting mixtures were analyzed by gel electrophoresis. As shown in the gel migration pattern (Fig. 8), only the free DNA migrated in the gel (lanes 2 and 4). In particular, in lane 4, where the ratio of DNA/NPs is higher, a thick band of unbound DNA is visible, while for the lower DNA/NPs ratio (lane 3) the migration of DNA was not detected, with stained DNA observed only in the well where the SiO$_2$NPs remained. This suggests that in this latter case (0.5 μg) nearly all the DNA adsorbed onto the NPs surface. This was also confirmed by the variation from the net positive charge of amine modified SiO$_2$NPs to the negative surface charge exhibited by the DNA/SiO$_2$NPs (Fig. 8B). We, therefore, investigated whether the ability of SiO$_2$NPs to bind DNA could be used to carry exogenous DNA through the cell membrane, to be expressed in the cells, leading to the silencing of a specific protein expression. The DNA/SiO$_2$NPs complex was incubated with a cell line that expresses green fluorescent protein (tGFP-HeLa cell line). We used SiO$_2$NPs at a concentration of 2.5 nM (this concentration was previously determined to be non-toxic). Gene silencing was monitored in transgenic living cells at 24, 48, 72 and 96 h after incubation with the DNA/NPs using confocal microscopy. As positive control experiments, cells were incubated with Lipofectamine 2000 and Fugene-6, two well-known transfection agents. tGFP transgenic cells showed high level of green fluorescence also after 96 h (Fig. 9A), while cells transfected with Lipofectamine 2000 (Fig. 9C) or Fugene-6 (Fig. 9D) after 96 h presented a strong silencing of tGFP expression (about 50% of cells were not fluorescent). On the other side, cells incubated with DNA/SiO$_2$NPs for 96 h showed a higher incidence of tGFP silencing (about 70%, see Fig. 9B). Interestingly, unlike the traditional transfection agents, no signs of cytotoxicity were observed, and after 96 h cells had a good morphology and viability (Fig. S7†).

In conclusion, our results indicate that monodisperse and stable SiO$_2$NPs, regardless of the size and surface charge, are biocompatible nanomaterials when used in a reasonable concentration range (up to 2.5 nM). These data have been confirmed in five cell lines, evaluating different cytoxicity parameters, namely viability, membrane integrity and generation of ROS, and testing prolonged incubation times (up to 96 h). The formation of protein/SiO$_2$NP complexes in the cell culture media was observed to significantly impact the cellular uptake. In fact, while nanoparticle internalization was strongly dependent on the NPs size, the formation of protein corona around the NPs led to a surface charge independent uptake. The absence of detectable toxic effects *in vitro* renders SiO$_2$NPs a promising material for biomedical applications. For this reason, we tested SiO$_2$NPs ability to act as transfection agent for gene delivery. SiO$_2$NPs proved to be excellent carrier of DNA with optimum transfection agent properties, leading to a slow, but incisive silencing of tGFP expression, without affecting cell viability, representing an effective alternative to common transfection agents. In the future, the assessment of the long-term toxicity of SiO$_2$NPs *in vivo*, as well as the investigation of their transfection ability in *in vivo* systems for gene therapy, will be of high interest.

Experimental methods

### Synthesis of SiO$_2$NPs in a ternary w/o microemulsion (25 nm)

The ternary microemulsion was composed of a surfactant, an organic solvent and water. 880 μL of Triton X-100 (FLUKA), 3.75 mL of cyclohexane (J. T. Baker), 170 μL of water, and 50 μL of TEOS (99%, Sigma Aldrich) were mixed together and stirred for 30 min. Then, 60 μL of NH$_4$OH (28–30%, Sigma Aldrich) were added to the microemulsion. The mixture was left to stir for 24 h. After the reaction was completed, acetone (J. T. Baker) was added to break the microemulsion. Nanoparticles were recovered by centrifugation (4500 rpm, 30 min, 25 °C) and the surfactant and the unreacted molecules were washed out from the resultant precipitate of SiO$_2$NPs sequentially, with butanol (Sigma Aldrich), iso-propanol (Carlo Erba Reagents), ethanol (J. T. Baker) and water. The ultrasonic treatment was used to
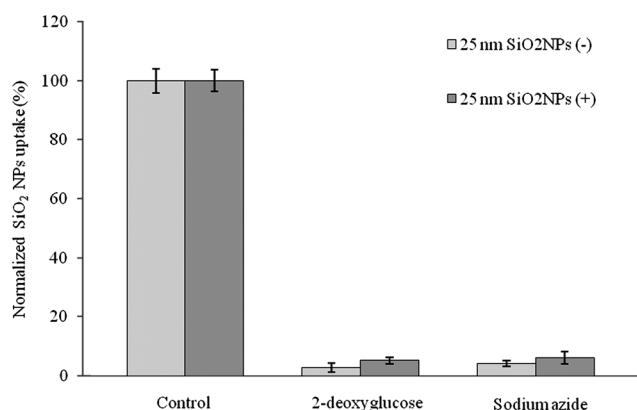
Fig. 7 Energy-dependent uptake of SiO$_2$NPs by A549 cells. Effects of two different inhibitory agents of endocytosis (2-deoxyglucose and sodium azide) on the uptake of SiO$_2$NPs with two surface charges (negative and positive) in A549 cells. Internalization data were expressed as the amount of internalized SiO$_2$NPs per cell (relative to control cells) after treatment with 100 μM inhibitors. Data were determined by ICP-AES (four independent experiments; error bars indicate the standard deviation).
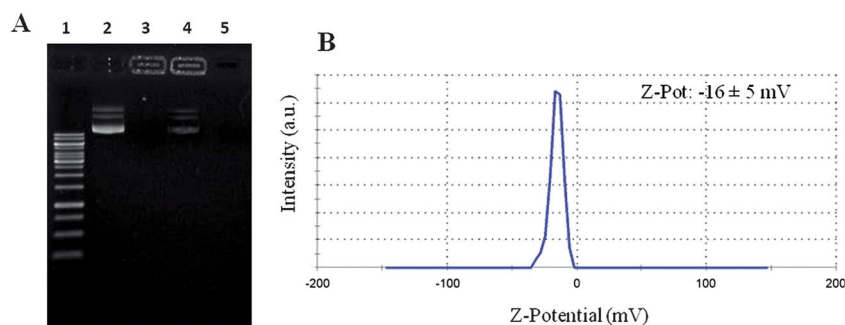
Fig. 8 (A) Representative gel showing the migration patterns of two quantities of plasmid DNA (0.5 and 2 μg) mixed with 200 μg of 25 nm amine modified SiO$_2$NPs after 40 min (100 V) of electrophoresis. Lane 1: DNA marker, lane 2: plasmid DNA, lane 3: SiO$_2$NPs mixed with 0.5 μg of DNA, lane 4: SiO$_2$NPs mixed with 2 μg of DNA, and lane 5: 25 nm amine modified SiO$_2$NPs. (B) ζ-Potential of SiO$_2$NPs mixed with 0.5 μg of DNA.
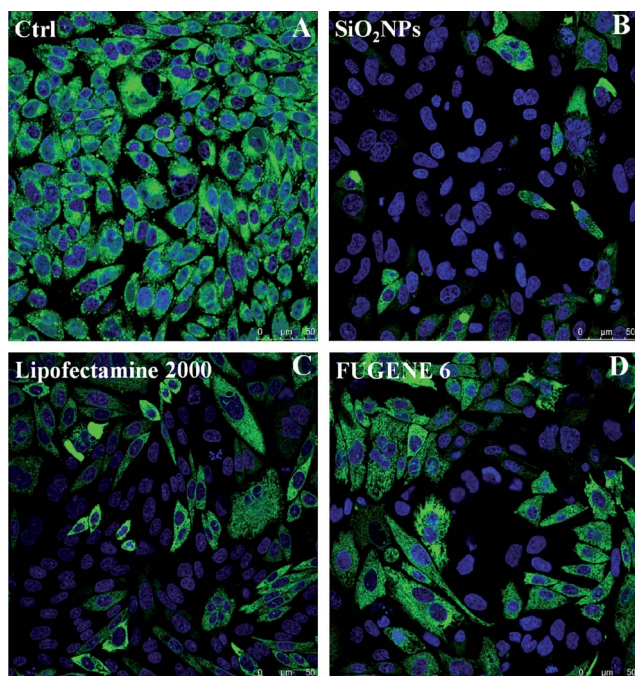
Fig. 9 Confocal images of green fluorescent HeLa cell lines. (A) Control sample after 96 h showed high level of green fluorescence; (B) cells incubated with 2.5 nM DNA/SiO$_2$NPs after 96 h showed a high incidence of silencing of tGFP expression (about 70% of fluorescence decrease); (C) cells transfected with Lipofectamine and (D) with Fugene-6 after 96 h typically showed 50% of cell silencing.

completely disperse the precipitate in the solvent and to remove the adsorbed molecules from the surface of the final product. The above-mentioned conditions yielded SiO$_2$NPs with a diameter of 25 nm. SiO$_2$NPs doped with QDs were obtained adding 2000 μmol of CdSe/ZnS QDs in chloroform before the addition of NH$_4$OH. TOP/TOPO capped CdSe/ZnS core/shell QDs were prepared by following standard colloidal synthesis procedures.[50,51]

Synthesis of SiO$_2$NPs in a quaternary w/o microemulsion (60 and 115 nm)

The quaternary w/o microemulsion was prepared at room temperature by mixing water, an organic solvent, a surfactant (Triton X-100) and a cosurfactant (hexanol for nanoparticles of 60 nm and butanol for those of 115 nm). In a typical procedure, 880 μL of Triton X-100, 3.75 mL of cyclohexane and 900 μL of hexanol (Sigma Aldrich) or butanol (Sigma Aldrich) were mixed together and stirred for 30 min. Then, 170 μL of water, 50 μL of TEOS and 30 μL of NH$_4$OH were added to the microemulsion. Subsequent steps were the same as those described for the 25 nm particles.

Preparation of amine-modified SiO$_2$NPs

SiO$_2$NPs were dispersed in a freshly prepared 5% (v/v) solution of aminopropyltriethoxysilane (APTES, Sigma Aldrich) and 1 mM acetic acid (99.7%, Sigma Aldrich) and stirred for 60 min³. After reaction, amine modified nanoparticles were separated by centrifugation (4500 rpm, 10 min), and washed 5–6 times with acetone and water (1 : 1). The nanoparticles were then redispersed in water.

TEM characterization

Transmission electron microscope (TEM) images were recorded by a JEOL JEM 1011 microscope operating at an accelerating voltage of 100 kV. TEM samples were prepared by dropping a dilute solution of nanoparticles in water on carbon-coated copper grids (Formvar/Carbon 300 Mesh Cu).

Photoluminescence/photoluminescence excitation (PL/PLE) measurements

Photoluminescence/photoluminescence excitation (PL/PLE) measurements of SiO$_2$NPs doped with QDs were recorded in photon counting mode by using a 450 W xenon lamp as the source of excitation and double monochromators both in excitation and emission. The emitted light was collected at right angles to the excitation radiation; excitation and emission bandwidths were 2 nm. Experiments were performed at room temperature (25 °C).

Dynamic light scattering (DLS) and ζ-potential measurements

Dynamic light scattering (DLS) and ζ-potential measurements were performed on a Zetasizer Nano ZS90 (Malvern, USA) equipped with a 4.0 mW HeNe laser operating at 633 nm and an

avalanche photodiode detector. Measurements were made at 25 °C in aqueous solutions (pH = 7).

Dynamic light scattering (DLS) and ζ-potential measurements upon incubation of NPs in cell culture medium

Cell culture medium DMEM high glucose (Dulbecco's Modified Eagle Medium) and RPMI-1640 (Rosenthal Park Memorial Institute) from Gibco Invitrogen were supplemented with 10% of Fetal Bovine Serum (FBS) (Gibco Invitrogen) as the protein source, with 50 μM glutamine (Gibco), 1 mM sodium pyruvate (Gibco), 100 U mL^{-1} penicillin and 100 mg mL^{-1} streptomycin (Invitrogen). Each size of SiO$_2$NPs was incubated at 37 °C with the two cell culture medium (RPMI or DMEM, 10% FBS) as previously described.[41] DLS and ζ-potential measurements were taken after 96 h of incubation after gently removing the protein excess.

Cell cultures

HeLa cells (human cervix carcinoma, IST cell bank, Interlab Cell Line Collection (ICLC) Accession number HTL95023), A549 cells (human lung carcinoma, HTL03001), and Caco-2 cells (human colon adenocarcinoma, HTL97023) were routinely cultivated in high glucose DMEM with 50 μM glutamine, supplemented with 10% FBS, 100 U mL^{-1} penicillin and 100 mg mL^{-1} streptomycin. U937 (IST cell factory, Genova, Italy) and Jurkat (human leukemia, HTL01002) were cultivated in RPMI 1640 with 50 μM glutamine, supplemented with 10% FBS, 100 U mL^{-1} penicillin and 100 mg mL^{-1} streptomycin. Fluorescent HeLa cells (LINTERNA™, Innoprot) were cultivated in high glucose DMEM with 50 μM glutamine, supplemented with 10% FBS and 250 mg L^{-1} G418 (Gibco). Cells were incubated in a humidified controlled atmosphere with a 95% to 5% ratio of air/CO$_2$, at 37 °C. The medium was changed every 3 days.

WST-8 assay

Adherent cells were seeded in 96 well microplates at a density of 5000 cells per well at a final volume of 50 μl and incubated for 24 h in a humidified atmosphere at 37 °C and 5% CO$_2$ to obtain a subconfluent monolayer (60–70% of confluence). Floating cells (Jurkat and U937 cells) were seeded in at the same conditions and immediately treated. SiO$_2$NPs were dispersed in the cell culture medium to attain stock solutions and added to the single well obtaining final SiO$_2$NP concentrations of 2.5, 25, 250, and 2500 pM (the 2500 pM concentration corresponds in mass unit to: 32, 450, and 3200 μg mL^{-1}, respectively for the 25, 60 and 115 nm SiO$_2$NPs) in a final volume of 100 μl for each well. The metabolic activity of all cell cultures was determined after 48 and 96 hours of exposure to 25, 60 and 115 nm SiO$_2$NPs, using a standard WST-8 assay (Sigma). 96 hours represent the maximum time in which cell viability is not influenced by deficiency of nutrients. Assays were performed in clear 96 well microplates (Sarstedt) for each time (48 and 96 hours). As a positive control for cytotoxicity, cells were incubated with 5% DMSO. 8 replicates were forecasted for each investigated point considering also controls (untreated cells) and blanks constituted by the addition of the medium only. 10 μl Cell Counting Reagent WST-8 (Sigma) was added to each well. The 96-well microplates

were placed in a humidified atmosphere of 5% CO$_2$ at 37 °C and incubated for 3 h. Subsequently, the orange WST-8 formazan product was measured by using a Fluo Star Optima (BMG LABTECH) microplate reader at a wavelength of 460 nm. Data were collected by Control Software and elaborated with MARS Data Analysis Software (BMG LABTECH). To express the cytotoxicity, the average absorbance of the wells containing cell culture medium without cells was subtracted from the average absorbance of the solvent control, 5% DMSO or SiO$_2$NPs treated cells. The percentage cell viability was calculated using the following equation:

$$(Absorbance_{treated}/Absorbance_{control}) \times 100\%$$

Data were expressed as mean ± SD. Differences in cell proliferation (WST-8) between cells treated with SiO$_2$NPs and the control were considered statistically significant performing a Student's t-test with a p-value of <0.05.

LDH assay

HeLa, U937, A549, Caco-2, and Jurkat cells were seeded in black 96 well microplates (Constar) and treated with three different sizes of SiO$_2$NPs with two surface charges at a final concentration of 2.5 nM, following the procedures reported for the WST-8 assay. After 96 hours of cell–NPs interaction, the lactate dehydrogenase (LDH) leakage assay was performed onto microplates by applying the CytoTox-ONE Homogeneous Membrane Integrity Assay reagent (Promega), following the manufacturer's instructions. LDH released in the extracellular environment was measured with a 10 minute coupled enzymatic assay that results in the conversion of resazurin into fluorescent resorufin (560Ex/590Em) by using a Fluo Star Optima (BMG LABTECH) microplate reader. As negative controls, we applied the same assay onto untreated cells. Results were normalized with respect to negative controls (expressed as 100%). Positive controls consisted in the treatment of cells with 0.9% Triton X-100. Data were expressed as mean ± SD. Differences in LDH leakage between cells treated with SiO$_2$NPs and controls were considered statistically significant performing a Student's t-test with a p-value of < 0.05.

DCF assay

HeLa, U937, A549, Caco-2, and Jurkat cells were seeded in 96-well microplates and treated with three sizes of SiO$_2$NPs with two surface charges at a final concentration of 2.5 nM. After 96 hours of cell–NPs interaction, the DCF-DA (2′,7′-dichlorofluorescein diacetate, Sigma) assay was performed onto microplates. On the day of the experiments, after removing the medium, the cells in the plates were washed with KRH buffer (Krebs Ringer HEPES buffer: 10 mM HEPES, 129 mM NaCl, 4.8 mM KCl, 1.2 mM KH$_2$PO$_4$, 5 mM NaHCO$_3$, 1 mM CaCl$_2$, 1.2 mM MgCl$_2$, 2.8 mM glucose, pH 7.4) and then incubated with 100 μM DCFH-DA in the loading medium (DMEM or RPMI 1640, 1% FBS). After the loading medium was removed, the cells were washed and incubated with KRH buffer and the fluorescence of the cells from each well was measured. DCFH-DA loaded cells were placed in a Fluo Star Optima (BMG LABTECH) microplate reader with temperature maintained at 37 °C. The excitation filter was set at

485 ± 6 nm and the emission filter was set at 530 ± 12.5 nm. As negative controls, we applied the same assay onto untreated cells. Results were normalized with respect to negative controls (expressed as 100%). As a positive control for cytotoxicity, cells were incubated with 500 μM H_2O_2. Data were expressed as mean ± SD. Differences in LDH leakage between cells treated with SiO_2NPs and controls were considered statistically significant performing a Student's t-test with a p-value of <0.05.

Determination of the intracellular uptake of SiO₂NPs by elemental analysis

Elemental analysis was carried out by inductively coupled plasma atomic emission spectroscopy (ICP-AES) with an Agilent 720/730 spectrometer. Samples were dissolved overnight in 1 mL of nitric acid, diluted to 5 mL with ultrapure water, and the resulting solution was directly analyzed. To estimate the intracellular Si concentration and hence the intracellular nanoparticle uptake, 10^5 cells were seeded in 1 mL of medium in each well (3.5 cm in diameter) of a 6-well plate. After 24 h of incubation at 37 °C, the medium was replaced with fresh medium containing the nanoparticles at a concentration of 2.5 nM. After 24 h of incubation at 37 °C, the medium was removed; the cells were washed three times with PBS (pH 7.4), trypsinized, and counted using a cell-counting chamber. Then, the cell suspensions were digested using nitric acid and the intracellular Si concentration was measured by means of elemental analysis and normalized to the number of cells.

Endocytosis inhibition experiments

A549 cells were seeded in 1 mL of medium in each well (3.5 cm in diameter) of a 6-well plate at a density of 10^5 cells per well and incubated for 24 h in a humidified atmosphere at 37 °C and 5% CO_2 to obtain a subconfluent monolayer (60–70% of confluence). After 24 h of incubation, the medium was removed, the cells were washed three times with PBS (pH 7.4), and replaced with fresh medium. To study the effect of various inhibitors on NPs uptake, cells were preincubated for 20 min at 37 °C with two inhibitors: sodium azide (100 μM) and 2-deoxyglucose (100 μM) and then with a suspension of SiO_2NPs (2.5 nM) for 1 h. As a control, cells were incubated with SiO_2NPs (2.5 nM) without inhibitors. After 1 h of incubation at 37 °C, the medium was removed; the cells were washed three times with PBS (pH 7.4), trypsinized, and counted using a cell-counting chamber. Then, the cell suspensions were digested using nitric acid, and the intracellular Si concentration was measured by means of ICP and normalized to the number of cells.

DNA binding experiment

SiO_2NPs of 25 nm functionalized with amine groups were mixed with a plasmid vector of 7087 base pairs that contains a shRNA sequence targeting TurboGFP (MISSION TurboGFP shRNA Control Vector, Sigma) in TBE (45 mM Tris, 45 mM boric acid and 1 mM EDTA). In particular, 200 μg of NPs were mixed with growing amount of plasmidic vector (0.5 μg and 2 μg) and incubated for 2 h. After incubation the NPs/DNA mixture was analyzed using 1% agarose gel in TBE buffer (45 mM Tris, 45 mM boric acid and 1 mM EDTA) containing SYBR Green

(Sigma). After 40 min (100 V) of electrophoresis, the gel was exposed on a UV transilluminator and the DNA quantified by a gel documentation system (Gel Doc XR, Biorad).

SiO₂NPs assisted transfection

One day before transfection, HeLa Linterna cells were seeded at a density of 10^5 cells per mL, in glass bottom Petri dishes (35 mm FluoroDish with a 10 mm well) using DMEM (Sigma) without antibiotics, to attain 90–95% confluence at the time of transfection. SiO_2NPs with DNA adsorbed onto the surface were prepared in Opti-MEM I (Invitrogen) with a final volume of 100 μl, containing 0.2 μg of DNA and 2.5 nM of SiO_2NPs; 100 μl of the mix were added to each well. These complexes were incubated with the cells and left for 5 h in serum free medium in order to avoid interaction of DNA/NPs complexes with serum proteins and to facilitate binding to the cell membrane. As negative controls, cells were incubated both with free DNA and SiO_2NPs. In all cases, transfection reagents were removed after 5 h of incubation and substituted with antibiotic free complete DMEM. Cells were left undisturbed for 24 h before confocal microscopy monitoring of tGFP silencing. Confocal images were taken at 24, 48, 72 and 96 h after the introduction of the reaction mixture. In parallel, lipotransfection was used as positive control. HeLa cells were transfected using two popular lipotransfection reagents, namely Lipofectamine 2000 (Invitrogen) and Fugene 6 (Roche). DNA–Lipofectamine complexes were prepared in Opti-MEM I with a final volume of 100 μl, containing 0.2 μg of DNA and 0.5 μl of transfection reagent, following the manufacturer instruction, 100 μl of the mix were added to each well. Moreover, green fluorescent HeLa cells were transfected in 100 μl wells using 0.3 μl Fugene 6 and 0.2 μg DNA, following the manufacturer instruction. Subsequent steps were the same as those described for the SiO_2NPs.

Confocal microscopy imaging of cells

Confocal microscopy images were recorded on a confocal microscope (Leica TCS-SP5 AOBS). A549 cells in DMEM were incubated with SiO_2NPs doped with QDs at a final concentration of 10 nM for 48 hours at 37 °C in 5% CO_2. Then, samples were washed with PBS pH 7.4 (Sigma), harvested and fixed in buffered 3.7% paraformaldehyde (Sigma) for 20 min, at 4 °C. For nuclear staining, cells were permeabilized for 20 min using 0.05% Triton X-100 in PBS, extensively washed with PBS, and labeled with Hoechst 33250 (1 nM in PBS) for 10 min.

References

1 J. Lu, M. Liong, S. Sherman, T. Xia, M. Kovochich, A. E. Nel, J. I. Zink and F. Tamanoi, *NanoBiotechnology*, 2007, **3**, 89–95.
2 C. Hom, J. Lu and F. Tamanoi, *J. Mater. Chem.*, 2009, **19**, 6308–6316.
3 M. Qhobosheane, S. Santra, P. Zhang and W. H. Tan, *Analyst*, 2001, **126**, 1274–1278.
4 G. Oberdorster, V. Stone and K. Donaldson, *Nanotoxicology*, 2007, **1**, 2–25.
5 D. Napierska, L. C. J. Thomassen, D. Lison, J. A. Martens and P. H. Hoet, *Part. Fibre Toxicol.*, 2010, **7**, 39.
6 B. Fadeel and A. E. Garcia-Bennett, *Adv. Drug Delivery Rev.*, 2010, **62**, 362–374.
7 R. K. Shukla, A. Kumar, A. K. Pandey, S. S. Singh and A. Dhawan, *J. Biomed. Nanotechnol.*, 2011,7, 100–101.

8   S. Halappanavar, P. Jackson, A. Williams, K. A. Jensen, K. S. Hougaard, U. Vogel, C. L. Yauk and H. Wallin, *Environ. Mol. Mutagen.*, 2011, 52, 425–439.

9   H. Haniu, Y. Matsuda, Y. Usui, K. Aoki, M. Shimizu, N. Ogihara, K. Hara, M. Okamoto, S. Takanashi, N. Ishigaki, K. Nakamura, H. Kato and N. Saito, *J. Proteomics*, 2011, 74, 2703–2712.

10 M. L. Di Giorgio, S. D. Bucchianico, A. M. Ragnelli, P. Aimola, S. Santucci and A. Poma, *Mutat. Res.*, 2011, 722, 20–31.

11 H. Vallhov, S. Gabrielsson, M. Stromme, A. Scheynius and A. E. Garcia-Bennett, *Nano Lett.*, 2007, 7, 3576–3582.

12 H. Ling, M. Zwengwei, Z. Yuying and G. Changyou, *Soft Nanosci. Lett.*, 2011, 1, 1–16.

13 D. Napierska, L. C. J. Thomassen, V. Rabolli, D. Lison, L. Gonzalez, M. Kirsch-Volders, J. A. Martens and P. H. Hoet, *Small*, 2009, 5, 846–853.

14 L. C. J. Thomassen, A. Aerts, V. Rabolli, D. Lison, L. Gonzalez, M. Kirsch-Volders, D. Napierska, P. H. Hoet, C. E. A. Kirschhock and J. A. Martens, *Langmuir*, 2010, 26, 328–335.

15 I. Fenoglio, G. Martra, S. Coluccia and B. Fubini, *Chem. Res. Toxicol.*, 2000, 13, 971–975.

16 K. M. Waters, L. M. Masiello, R. C. Zangar, R. C. Zangar, N. J. Karin, R. D. Quesenberry, S. Bandyopadhyay, J. G. Teeguarden, J. G. Pounds and B. D. Thrall, *Toxicol. Sci.*, 2009, 107, 553–569.

17 R. S. Pandurangi, M. S. Seehra, B. L. Razzaboni and P. Bolsaitis, *Environ. Health Perspect.*, 1990, 86, 327–336.

18 V. Murashov, M. Harper and E. Demchuk, *J. Occup. Environ. Hyg.*, 2006, 3, 718–723.

19 B. Fubini and A. Hubbard, *Free Radical Biol. Med.*, 2003, 34, 1507–1516.

20 M. Horie, K. Nishio, K. Fujita, S. Endoh, A. Miyauchi, Y. Saito, H. Iwahashi, K. Yamamoto, H. Murayama, H. Nakano, N. Nanashima, E. Niki and Y. Yoshida, *Chem. Res. Toxicol.*, 2009, 22, 543–553.

21 W. Shang, J. H. Nuffer, V. A. Muniz-Papandrea, W. Colon, R. W. Siegel and J. S. Dordick, *Small*, 2009, 5, 470–476.

22 I. Slowing, B. G. Trewyn and V. S. Lin, *J. Am. Chem. Soc.*, 2006, 128, 14792–14793.

23 B. Diaz, C. Sanchez-Espinel, M. Arruebo, J. Faro, E. de Miguel, S. Magadan, C. Yague, R. Fernandez-Pacheco, M. R. Ibarra, J. Santamaria and A. Gonzalez-Fernandez, *Small*, 2008, 4, 2025–2034.

24 S. K. Sohaebuddin, P. T. Thevenot, D. Baker, J. W. Eaton and L. P. Tang, *Part. Fibre Toxicol.*, 2010, 7, 22.

25 V. Rabolli, L. C. Thomassen, C. Princen, D. Napierska, L. Gonzalez, M. Kirsch-Volders, P. H. Hoet, F. Huaux, C. E. Kirschhock, J. A. Martens and D. Lison, *Nanotoxicology*, 2010, 4, 307–318.

26 C. M. Sayes and D. B. Warheit, *Wiley Interdiscip. Rev. Nanomed. Nanobiotechnol.*, 2009, 1, 660–670.

27 N. A. Monteiro-Riviere, A. O. Inman and L. W. Zhang, *Toxicol. Appl. Pharmacol.*, 2009, 234, 222–235.

28 J. Lu, M. Liong, Z. Li, J. I. Zink and F. Tamanoi, *Small*, 2010, 6, 1794–1805.

29 J. L. Vivero-Escoto, I. I. Slowing, B. G. Trewyn and V. S. Lin, *Small*, 2010, 6, 1952–1967.

30 L. Li, F. Tang, H. Liu, T. Liu, N. Hao, D. Chen, X. Teng and J. He, *ACS Nano*, 2010, 4, 6874–6882.

31 I. Abarkan, T. Doussineau and M. Smaihi, *Polyhedron*, 2006, 25, 1763–1770.

32 Y. Ye, J. Liu, J. Xu, L. Sun, M. Chen and M. Lan, *Toxicol. In Vitro*, 2010, 24, 751–758.

33 P. Mukherjee, R. R. Arvizo, O. R. Miranda, M. A. Thompson, C. M. Pabelick, R. Bhattacharya, J. D. Robertson, V. M. Rotello and Y. S. Prakash, *Nano Lett.*, 2010, 10, 2543–2548.

34 Y. Hung, T. H. Chung, S. H. Wu, M. Yao, C. W. Lu, Y. S. Lin, C. Y. Mou, Y. C. Chen and D. M. Huang, *Biomaterials*, 2007, 28, 2959–2966.

35 S. H. Wang, C. W. Lee, A. Chiou and P. K. Wei, *J. Nanobiotechnol.*, 2010, 8, 33.

36 C. Y. Mou, F. Lu, S. H. Wu and Y. Hung, *Small*, 2009, 5, 1408–1413.

37 N. M. Schaeublin, L. K. Braydich-Stolle, A. M. Schrand, J. M. Miller, J. Hutchison, J. J. Schlager and S. M. Hussain, *Nanoscale*, 2011, 3, 410–420.

38 T. Yu, A. Malugin and H. Ghandehari, *ACS Nano*, 2011, 5, 5715–5728.

39 M. Lundqvist, J. Stigler, G. Elia, I. Lynch, T. Cedervall and K. A. Dawson, *Proc. Natl. Acad. Sci. U. S. A.*, 2008, 105, 14265–14270.

40 T. Cedervall, I. Lynch, S. Lindman, T. Berggard, E. Thulin, H. Nilsson, K. A. Dawson and S. Linse, *Proc. Natl. Acad. Sci. U. S. A.*, 2007, 104, 2050–2055.

41 G. Maiorano, S. Sabella, B. Sorce, V. Brunetti, M. A. Malvindi, R. Cingolani and P. P. Pompa, *ACS Nano*, 2010, 4, 7481–7491.

42 D. Dutta, S. K. Sundaram, J. G. Teeguarden, B. J. Riley, L. S. Fifield, J. M. Jacobs, S. R. Addleman, G. A. Kaysen, B. M. Moudgil and T. J. Weber, *Toxicol. Sci.*, 2007, 100, 303–315.

43 H. C. Lichstein and M. H. Soule, *J. Bacteriol.*, 1944, 47, 253–257.

44 A. Verma, O. Uzun, Y. H. Hu, Y. Hu, H. S. Han, N. Watson, S. L. Chen, D. J. Irvine and F. Stellacci, *Nat. Mater.*, 2008, 7, 588–595.

45 P. Huang, H. Pelicano, D. S. Martin and R. H. Xu, *Oncogene*, 2006, 25, 4633–4646.

46 Z. Chu, Y. Huang, Q. Tao and Q. Li, *Nanoscale*, 2011, 3, 3291–3299.

47 R. M. Schiffelers, A. Ansari, J. Xu, Q. Zhou, Q. Tang, G. Storm, G. Molema, P. Y. Lu, P. V. Scaria and M. C. Woodle, *Nucleic Acids Res.*, 2004, 32, e149.

48 C. Zhang, J. T. Newsome, R. Mewani, J. Pei, P. C. Gokhale and U. N. Kasid, *Methods Mol. Biol. (N. Y., NY, U. S.)*, 2009, 480, 65–83.

49 G. Bardi, M. A. Malvindi, L. Gherardini, M. Costa, P. P. Pompa, R. Cingolani and T. Pizzorusso, *Biomaterials*, 2010, 31, 6555–6566.

50 B. O. Dabbousi, J. RodriguezViejo, F. V. Mikulec, J. R. Heine, H. Mattoussi, R. Ober, K. F. Jensen and M. G. Bawendi, *J. Phys. Chem. B*, 1997, 101, 9463–9475.

51 Z. A. Peng and X. G. Peng, *J. Am. Chem. Soc.*, 2001, 123, 183–184.